Improving Weak Gravitational Lensing

Using Kinematic Information from Galaxies

Jordy Ram[1]

Supervisors: Prof. Dr. Martin Kilbinger[1,2] **& Dr. Cail Daley**[2]

[1]Université Paris-Saclay [2]CEA Saclay/IRFU/DAp

July 6, 2025

Traditional Weak Lensing

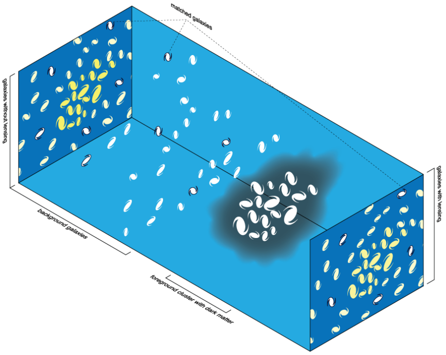

Figure 1: (M. Sachs, 2008).

Concept:

- Small distortions in galaxy shapes due to matter distribution in the line of sight
- The intrinsic galaxy shapes are unknown
- Need to average over a significant number of galaxies to measure the distortion

Traditional Weak Lensing

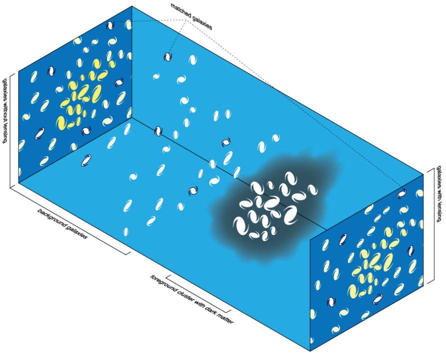

Figure 1: (M. Sachs, 2008).

Concept:

- Small distortions in galaxy shapes due to matter distribution in the line of sight
- The intrinsic galaxy shapes are unknown
- Need to average over a significant number of galaxies to measure the distortion

Traditional Weak Lensing

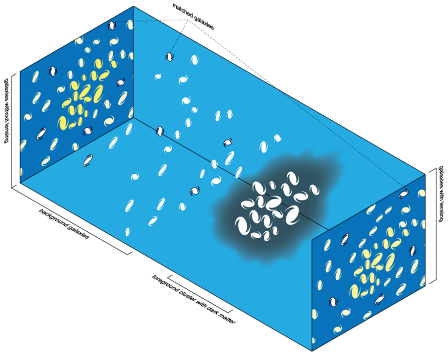

Figure 1: (M. Sachs, 2008).

Concept:

- Small distortions in galaxy shapes due to matter distribution in the line of sight
- The intrinsic galaxy shapes are unknown
- Need to average over a significant number of galaxies to measure the distortion

Kinematic Weak Lensing

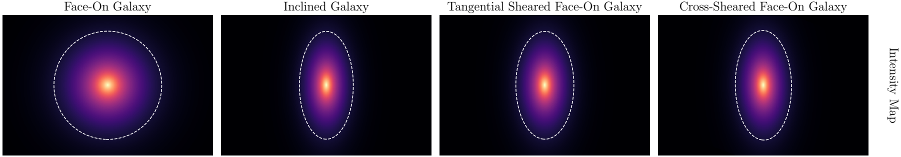

Kinematic Weak Lensing

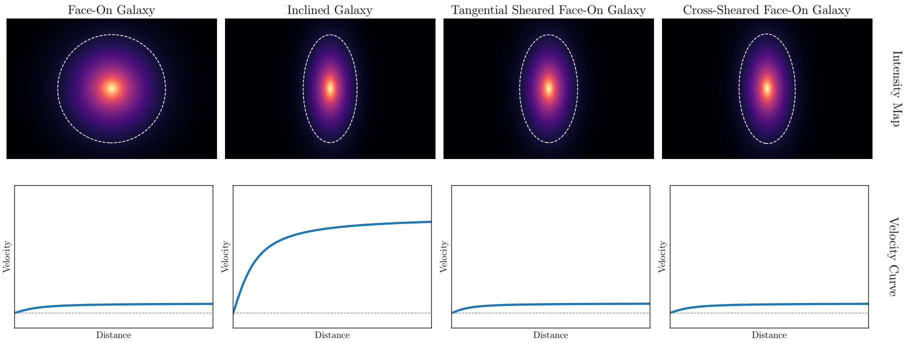

Kinematic Weak Lensing

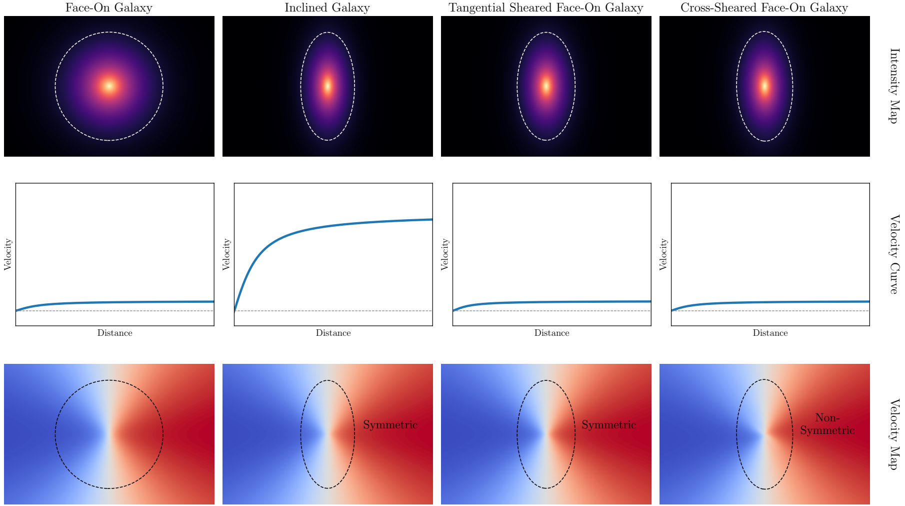

Velocity Fields of Disk Galaxies

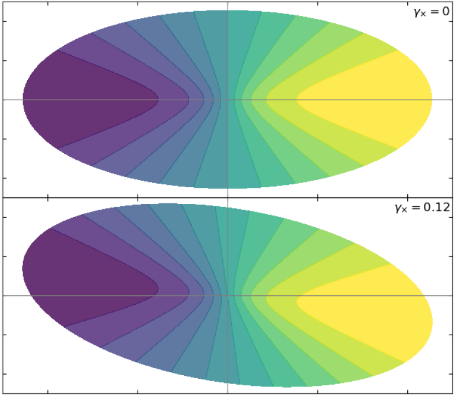

Figure 2: Velocity field of a non-sheared and sheared galaxy [1]

Characteristics when $\gamma_\times = 0$:

- Symmetry around the major axis
- Antisymmetry around the minor axis

Characteristics when $\gamma_\times = 0.12$:

- Broken reflection symmetries

Velocity Fields of Disk Galaxies

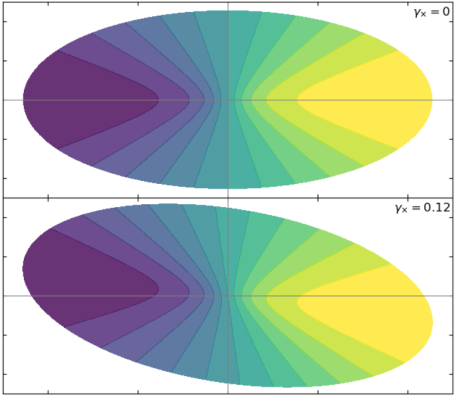

Figure 2: Velocity field of a non-sheared and sheared galaxy [1]

Characteristics when $\gamma_\times = 0$:

- Symmetry around the major axis
- Antisymmetry around the minor axis

Characteristics when $\gamma_\times = 0.12$:

- Broken reflection symmetries

Model-Independent Restoration of Reflection Symmetries

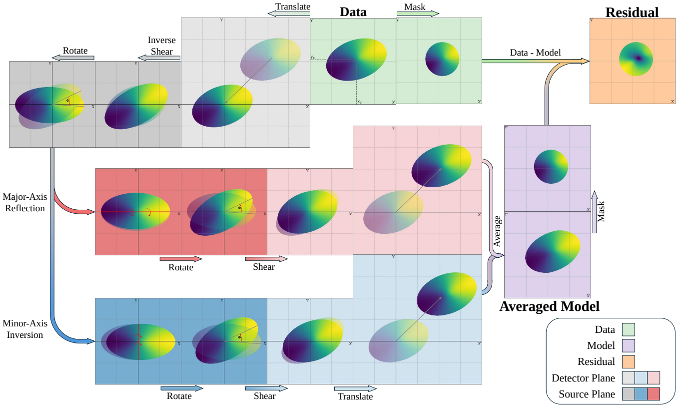

Figure 3: MIRoRS Algorithm. [1]

Fitting Parameters

Parameter	Symbol
Shear	$\gamma_\times$
Central Velocity	V_c
Position Angle	ϕ
Centroid	(x_c, y_c)

Table 1

Shear Estimation using MIRoRS and MCMC

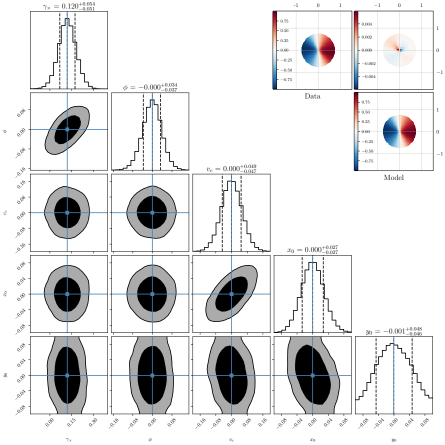

Figure 4

MCMC (Markov Chain Monte Carlo)

- Provides probability distributions of multiple parameters

Observation:

- Estimated shear value is equal to the true shear value, $\gamma_\times = 0.12$

Shear Estimation using MIRoRS and MCMC

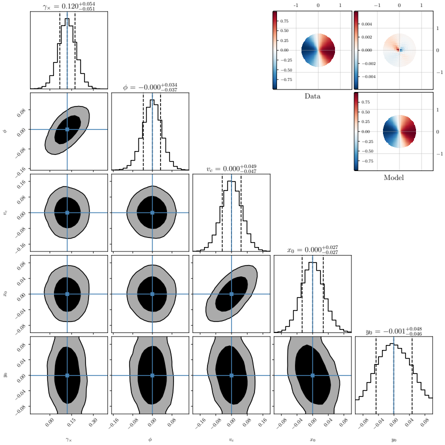

Figure 4

MCMC (Markov Chain Monte Carlo)

- Provides probability distributions of multiple parameters

Observation:

- Estimated shear value is equal to the true shear value, $\gamma_\times = 0.12$

Degeneracy at Position Angle of 45 degrees

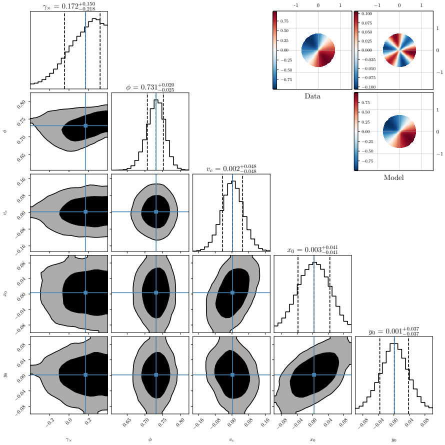

Figure 5

Observation:

- If the galaxy is at $\phi = 45^\circ$ in the observer's frame, $\gamma_\times$ manifest as γ_+, which does not change the symmetry.

Approach:

- Determining the cross-shear in the galaxy frame

Degeneracy at Position Angle of 45 degrees

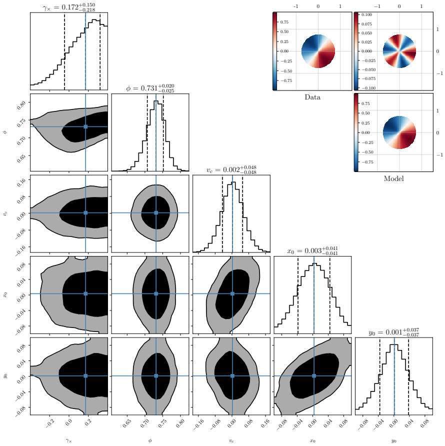

Figure 5

Observation:

- If the galaxy is at $\phi = 45^\circ$ in the observer's frame, $\gamma_\times$ manifest as γ_+, which does not change the symmetry.

Approach:

- Determining the cross-shear in the galaxy frame

Improving the MIRoRS Method

Shear Matrix in Current MIRoRS

$$\mathcal{A} = \begin{pmatrix} 1 & -\gamma_\times \\ -\gamma_\times & 1 \end{pmatrix}. \quad (1)$$

Transformation to Galaxy Frame:
Decompose $\gamma_\times$ into a tangential and cross component

Shear Matrix in Novel MIRoRS

$$\gamma_1 = \gamma_\times \cdot \sin(2\phi) \quad (2)$$

$$\gamma_2 = \gamma_\times \cdot \cos(2\phi). \quad (3)$$

$$\mathcal{A} = \begin{pmatrix} 1-\gamma_1 & -\gamma_2 \\ -\gamma_2 & 1+\gamma_1 \end{pmatrix} \quad (4)$$

Improving the MIRoRS Method

Shear Matrix in Current MIRoRS

$$\mathcal{A} = \begin{pmatrix} 1 & -\gamma_\times \\ -\gamma_\times & 1 \end{pmatrix}. \tag{1}$$

Transformation to Galaxy Frame:
Decompose $\gamma_\times$ into a tangential and cross component

Shear Matrix in Novel MIRoRS

$$\gamma_1 = \gamma_\times \cdot \sin(2\phi) \tag{2}$$

$$\gamma_2 = \gamma_\times \cdot \cos(2\phi). \tag{3}$$

$$\mathcal{A} = \begin{pmatrix} 1-\gamma_1 & -\gamma_2 \\ -\gamma_2 & 1+\gamma_1 \end{pmatrix} \tag{4}$$

Improving the MIRoRS Method

Shear Matrix in Current MIRoRS

$$\mathcal{A} = \begin{pmatrix} 1 & -\gamma_\times \\ -\gamma_\times & 1 \end{pmatrix}. \qquad (1)$$

Transformation to Galaxy Frame:
Decompose $\gamma_\times$ into a tangential and cross component

Shear Matrix in Novel MIRoRS

$$\gamma_1 = \gamma_\times \cdot \sin(2\phi) \qquad (2)$$

$$\gamma_2 = \gamma_\times \cdot \cos(2\phi). \qquad (3)$$

$$\mathcal{A} = \begin{pmatrix} 1-\gamma_1 & -\gamma_2 \\ -\gamma_2 & 1+\gamma_1 \end{pmatrix} \qquad (4)$$

Applying MIRoRS to Simulated Galaxy Data

MaNGIA (Mapping Nearby Galaxies with IllustrisTNG Astrophysics):

- 10,000 mock MaNGA galaxies

Velocity Field:

- Velocity provided in fibers distributed in a hexagonal pattern

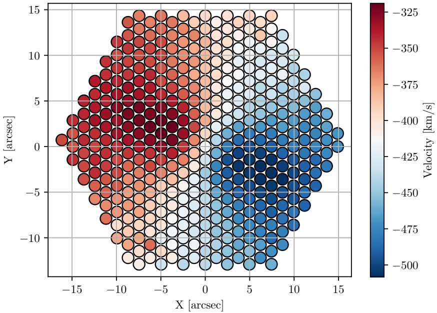

Figure 6: Simulated velocity field.

Applying MIRoRS to Simulated Galaxy Data

MaNGIA (Mapping Nearby Galaxies with IllustrisTNG Astrophysics):

- 10,000 mock MaNGA galaxies

Velocity Field:

- Velocity provided in fibers distributed in a hexagonal pattern

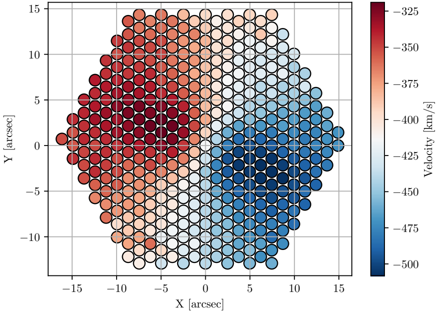

Figure 6: Simulated velocity field.

Angle Dependence of Shear Estimation

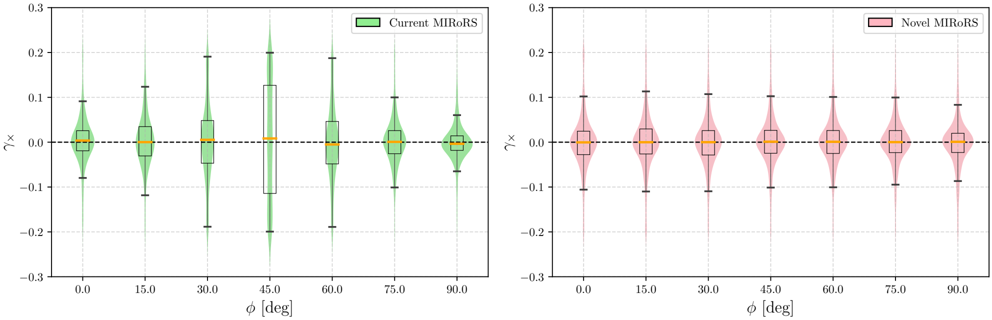

Figure 7: The deviation from the true cross-shear for different galaxy position angles.

- Degeneracy at $\phi = 45°$ disappears completely in novel MIRoRS method

Angle Dependence of Shear Estimation

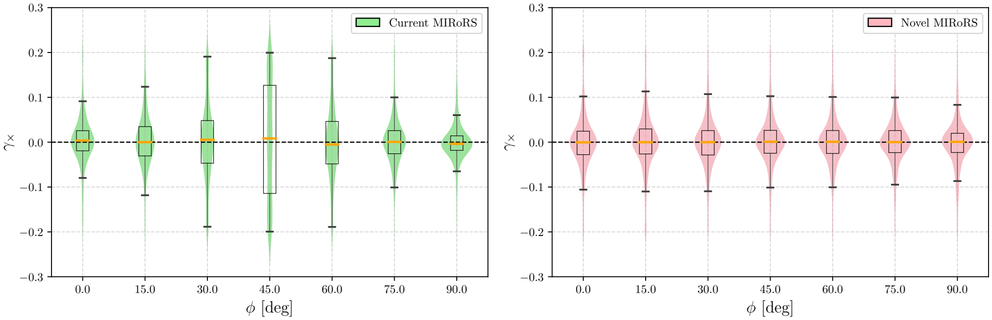

Figure 7: The deviation from the true cross-shear for different galaxy position angles.

- Degeneracy at $\phi = 45^\circ$ disappears completely in novel MIRoRS method

Symmetry in Velocity Fields of Elliptical Galaxies

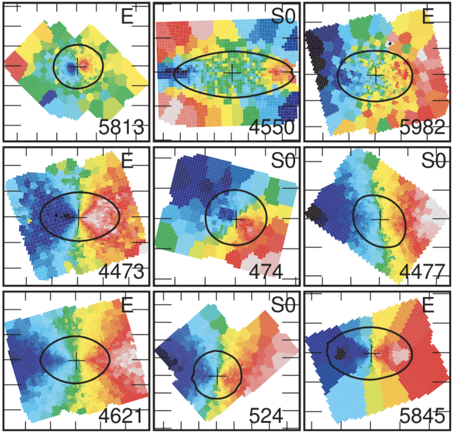

Figure 8: Observed Velocity Fields [2].

Interesting Observation:

- Velocity fields from elliptical galaxies show symmetry

Crucial Questions:

- Can the MIRoRS method be applied to elliptical galaxies?
- What are the implications of this?

Symmetry in Velocity Fields of Elliptical Galaxies

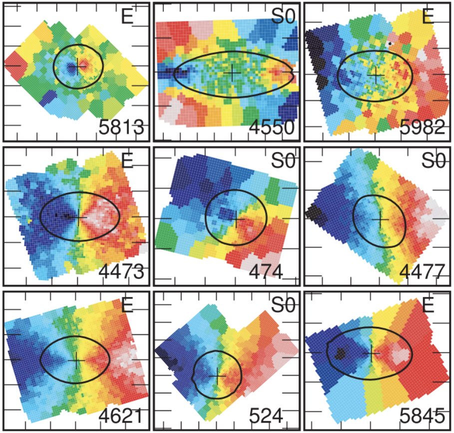

Figure 8: Observed Velocity Fields [2].

Interesting Observation:

- Velocity fields from elliptical galaxies show symmetry

Crucial Questions:

- Can the MIRoRS method be applied to elliptical galaxies?
- What are the implications of this?

université PARIS-SACLAY
FACULTÉ DES SCIENCES D'ORSAY

Symmetry in Velocity Fields of Elliptical Galaxies

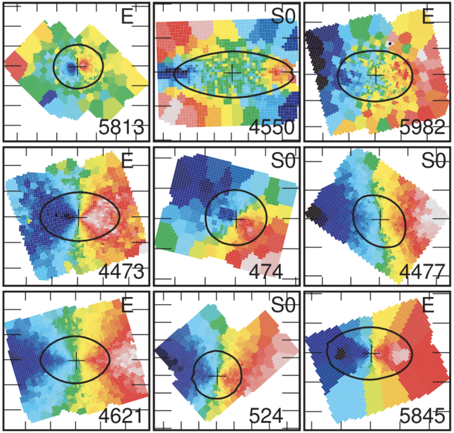

Figure 8: Observed Velocity Fields [2].

Interesting Observation:

- Velocity fields from elliptical galaxies show symmetry

Crucial Questions:

- Can the MIRoRS method be applied to elliptical galaxies?
- What are the implications of this?

Selecting Elliptical Galaxies

1 Ratio of Rotation Velocity and Velocity Dispersion

$$\frac{V}{\sigma} = \frac{\sqrt{\left\langle \left(V_{\text{centered}}\right)^2 \right\rangle}}{\sqrt{\langle \sigma^2 \rangle}} \tag{5}$$

2 Specific Star-Formation Rate

$$sSFR = \frac{SFR}{M_*} \tag{6}$$

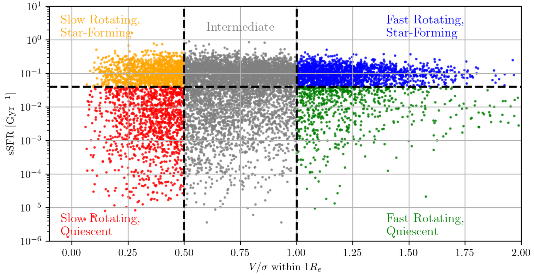

Figure 9: Classification of MaNGIA Galaxies

Selecting Elliptical Galaxies

1 Ratio of Rotation Velocity and Velocity Dispersion

$$\frac{V}{\sigma} = \frac{\sqrt{\left\langle \left(V_{\text{centered}}\right)^2 \right\rangle}}{\sqrt{\langle \sigma^2 \rangle}} \quad (5)$$

2 Specific Star-Formation Rate

$$sSFR = \frac{SFR}{M_*} \quad (6)$$

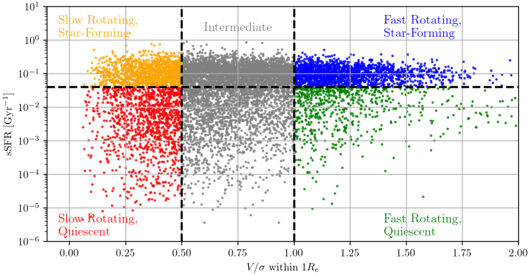

Figure 9: Classification of MaNGIA Galaxies

Cross-Shear per Galaxy Type

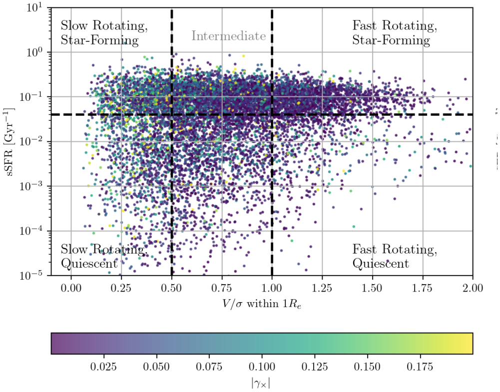

Figure 10: Cross-shear and its statistical significance per galaxy type

Observation:

- Random scatter: No obvious dependence of cross-shear on galaxy type

Cross-Shear for Ellipticals and Disk Galaxies

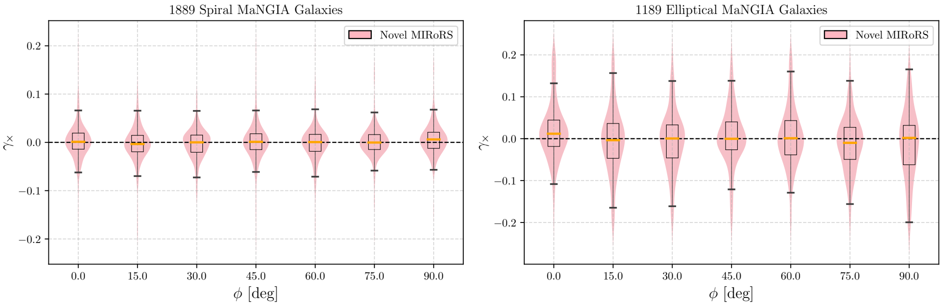

Figure 11: The deviation from the true cross-shear for different galaxy position angles.

- Elliptical galaxies consistent with $\gamma_\times = 0$ for all position angles

universite PARIS-SACLAY
FACULTÉ DES SCIENCES D'ORSAY

Cross-Shear for Ellipticals and Disk Galaxies

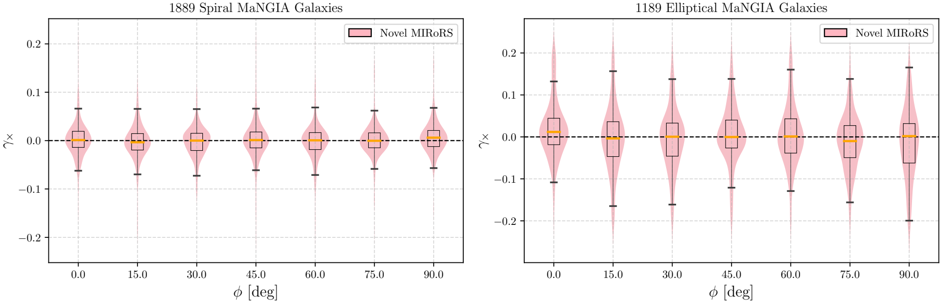

Figure 11: The deviation from the true cross-shear for different galaxy position angles.

- Elliptical galaxies consistent with $\gamma_\times = 0$ for all position angles

Probability Distributions per Galaxy Type

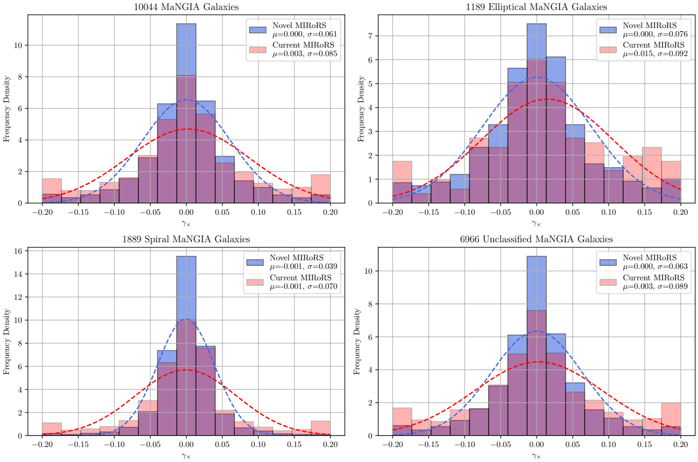

Figure 12: Probability distributions of cross-shear per galaxy type

Conclusions & Future Research

Conclusion:

- Kinematic lensing is expected to reduce the variance from shape noise
- Tested MIRoRS, along with an improved method, on MaNGIA mock galaxies in the Illustris TNG simulation
- **Comparable shear constraints can be achieved with disk and elliptical galaxies, potentially increasing the number of galaxies that can be used with this kinematic lensing method**

Future Research:

- Using more realistic velocity maps

Conclusions & Future Research

Conclusion:

- Kinematic lensing is expected to reduce the variance from shape noise
- Tested MIRoRS, along with an improved method, on MaNGIA mock galaxies in the Illustris TNG simulation
- Comparable shear constraints can be achieved with disk and elliptical galaxies, potentially increasing the number of galaxies that can be used with this kinematic lensing method

Future Research:

- Using more realistic velocity maps

Conclusions & Future Research

Conclusion:

- Kinematic lensing is expected to reduce the variance from shape noise
- Tested MIRoRS, along with an improved method, on MaNGIA mock galaxies in the Illustris TNG simulation
- **Comparable shear constraints can be achieved with disk and elliptical galaxies, potentially increasing the number of galaxies that can be used with this kinematic lensing method**

Future Research:

- Using more realistic velocity maps

Conclusions & Future Research

Conclusion:

- Kinematic lensing is expected to reduce the variance from shape noise
- Tested MIRoRS, along with an improved method, on MaNGIA mock galaxies in the Illustris TNG simulation
- **Comparable shear constraints can be achieved with disk and elliptical galaxies, potentially increasing the number of galaxies that can be used with this kinematic lensing method**

Future Research:

- Using more realistic velocity maps

Thank you for your attention!

References

[1] C. Hopp and D. Wittman, "Improving Precision in Kinematic Weak Lensing with MIRoRS: Model-Independent Restoration of Reflection Symmetries,", Sep. 2024. arXiv: 2410.00098 [astro-ph.CO].

[2] E. Emsellem, M. Cappellari, D. Krajnovi, *et al.*, "The SAURON project - IX. A kinematic classification for early-type galaxies," *Monthly Notices of the Royal Astronomical Society*, vol. 379, no. 2, pp. 401–417, Jul. 2007. DOI: 10.1111/j.1365-2966.2007.11752.x. [Online]. Available: https://doi.org/10.1111/j.1365-2966.2007.11752.x.

[3] ESA, *What Euclid will measure: Weak lensing*, May 2023. [Online]. Available: https://www.esa.int/ESA_Multimedia/Images/2023/05/What_Euclid_will_measure_weak_lensing.

Strong and Weak Gravitational Lensing

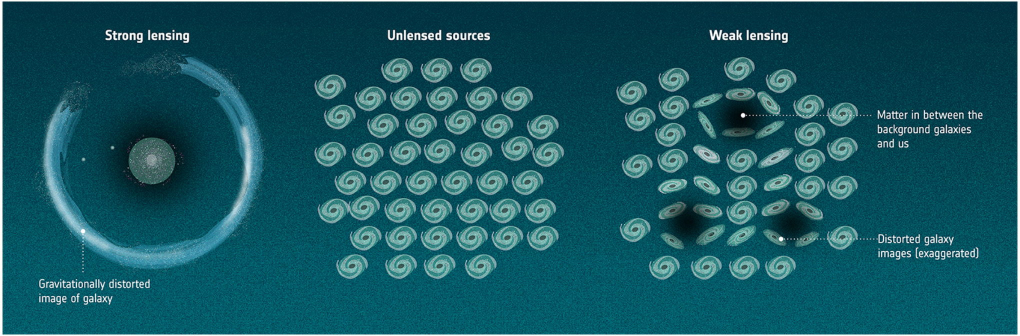

Figure 13: The concept of both strong gravitational lensing (on the left) and weak gravitational lensing (on the right) applied to a certain number of galaxies (in the center). Figure taken from [3]

Observed Ellipticities of Galaxies

The observed ellipticity of a galaxy is given by

$$\hat{\epsilon}^{obs} \approx \epsilon^{int} + \gamma, \tag{7}$$

The intrinsic galaxy shape is thus given by

$$\epsilon^{int} \approx \epsilon^{o} + \epsilon^{IA}, \tag{8}$$

Kinematic Lensing using Tully-Fischer

The intrinsic galaxy ellipticity at a certain disk inclination i is given by

$$\varepsilon^{int} = \frac{1 - \sqrt{1 - (1 - q_z^2)\sin^2 i}}{1 + \sqrt{1 - (1 - q_z^2)\sin^2 i}},$$

The inclination of the disk galaxy is given by

$$\sin i = \frac{v_{\text{major}}}{v_{\text{circ}}}, \tag{9}$$

The timate of the circular velocity is given by

$$\log \hat{v}_{circ} = \log v_{TF} = b\left(M_B - M_p\right) + a, \tag{10}$$

The measured shear in Kinematic Lensing is given by

$$\hat{\gamma} \equiv \hat{\epsilon}^{obs} - \hat{\epsilon}^{int}, \tag{11}$$

Operations

Inverse shear and counter-clockwise rotation matrices are given by [1]

$$\mathcal{A}^{-1} = \mu \begin{pmatrix} 1 & \gamma_\times \\ \gamma_\times & 1 \end{pmatrix}, \quad \mathcal{R}^{-1} = \begin{pmatrix} \cos\phi & \sin\phi \\ -\sin\phi & \cos\phi \end{pmatrix}, \tag{12}$$

Matrices for reflection under the major and minor axis are given by [1]

$$\mathcal{T}_x = \begin{pmatrix} 1 & 0 \\ 0 & -1 \end{pmatrix}, \qquad \mathcal{T}_y = \begin{pmatrix} -1 & 0 \\ 0 & 1 \end{pmatrix}. \tag{13}$$

Clockwise rotation and shear matrices are given by [1]

$$\mathcal{R} = \begin{pmatrix} \cos\phi & -\sin\phi \\ \sin\phi & \cos\phi \end{pmatrix}, \quad \mathcal{A} = \begin{pmatrix} 1 & -\gamma_\times \\ -\gamma_\times & 1 \end{pmatrix}. \tag{14}$$

Example Velocity Fields

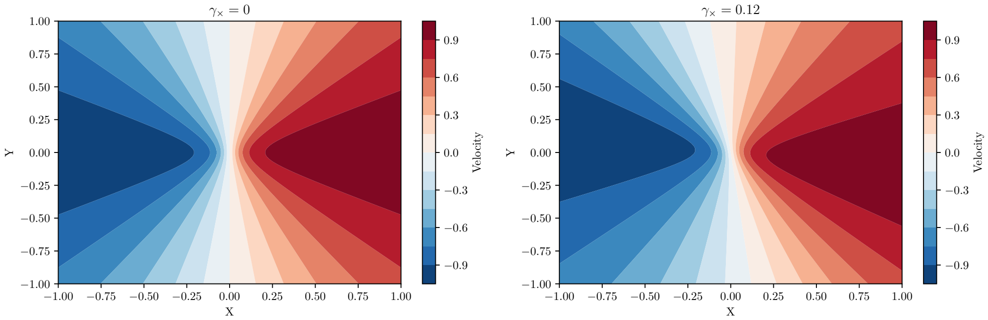

Figure 14: The unmasked velocity field of an unsheared galaxy (on the left) and the unmasked velocity field of a galaxy that is sheared using $\gamma_\times = 0.12$ (on the right). Both the galaxy position values and the velocity values have arbitrary units.

Photometric and Kinematic Axes

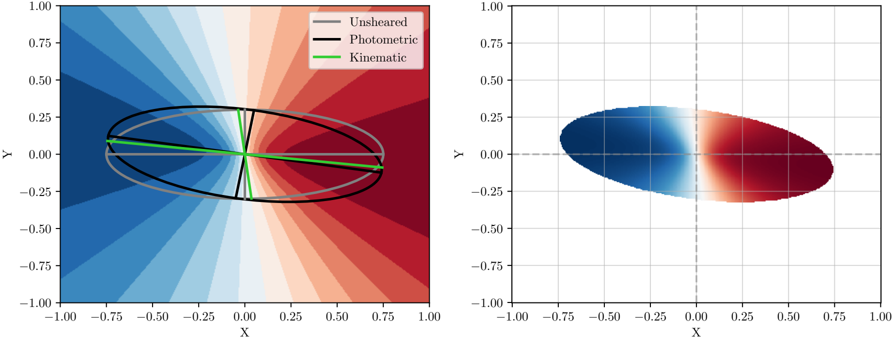

Figure 15: On the left side of the figure, the unmasked velocity field is shown with the unsheared galaxy isophote and its axis (in grey), and the galaxy isophote after lensing, including the photometric axis (in black), and the kinematic axis (in green). On the right side of the figure, the masked velocity field of the galaxy is shown.

Residual and χ^2 Maps

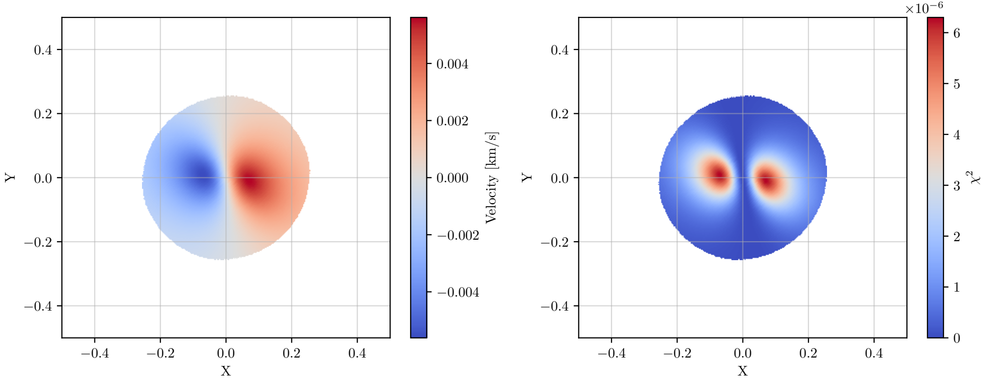

Figure 16: The residual velocity map (on the left), which is the difference between the observational velocity map and the velocity map from the model, and the corresponding χ^2-per-pixel map (on the right).

Likelihood Functions

The χ_i^2-values are given by

$$\chi_i^2 = \frac{\left(V_{i,\,\text{model}} - V_{i,\,\text{data}}\right)^2}{\sigma_i^2} = \frac{V_{i,\text{res}}^2}{\sigma_i^2}, \tag{15}$$

The likelihood function is given by

$$\mathcal{L} = \prod_i \frac{1}{\sqrt{2\pi\sigma_i^2}} e^{-\chi_i^2/2} \tag{16}$$

The log-likelihood is given by

$$\ln \mathcal{L} = -\frac{1}{2} \sum \left(\chi_i^2 + \ln \sigma_i^2 + \ln 2\pi\right) \tag{17}$$

Applying MIRoRS on Idealised Mock Galaxy

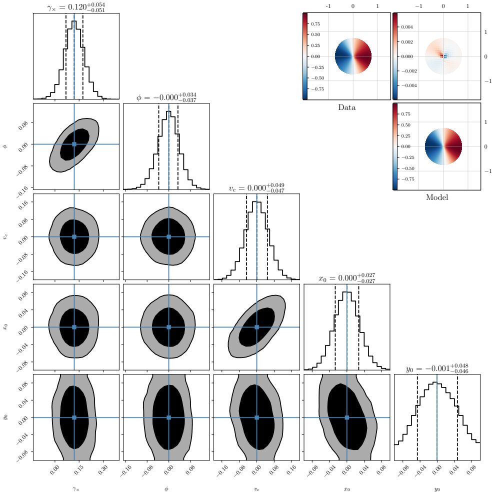

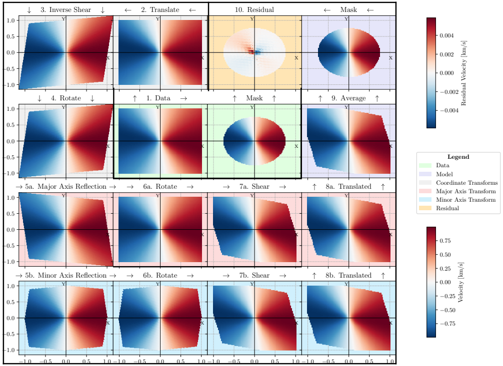

Figure 18

MCMCs for Rotated Idealised Mock Galaxy

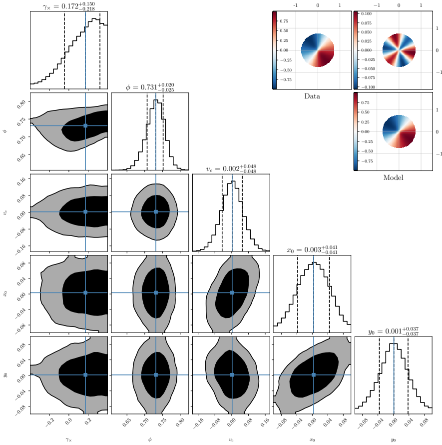

Figure 19: Current MIRoRS

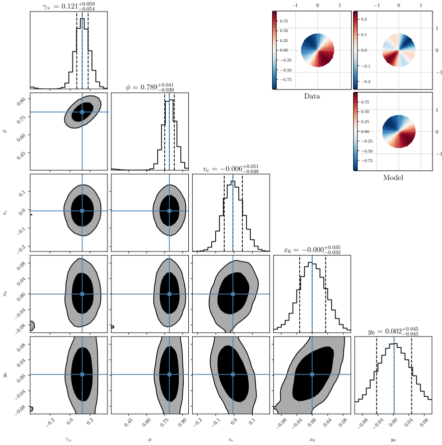

Figure 20: Novel MIRoRS

Velocity Grid and Interpolation

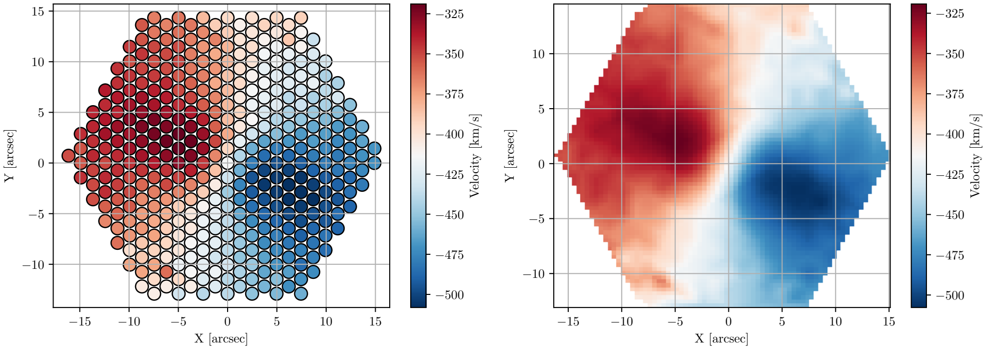

Figure 21: The velocities measured by the spectral lines in several mock datacubes (on the left), and the resulting extrapolated velocity field (on the right). The spatial coordinates of the mock galaxy are given in arc seconds, and the velocity is given in kilometers per second.

Determining the Optimal Mask Radius

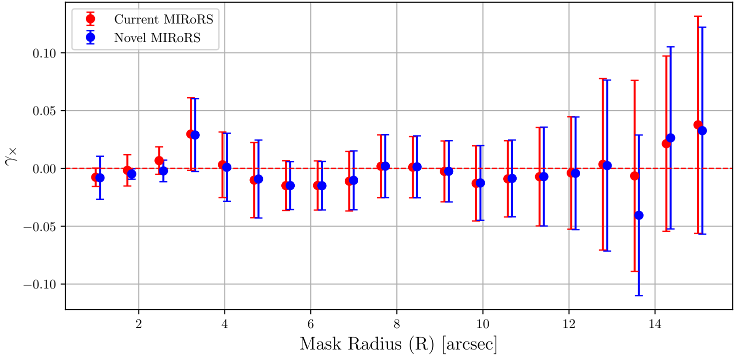

Figure 22: The average shear and its standard deviation calculated for several galaxies for different radii of the mask, which is applied to the data and model using the existing MIRoRS method (red) and the slightly adjusted method (blue).

Applying MIRoRS to MaNGIA Velocity Field

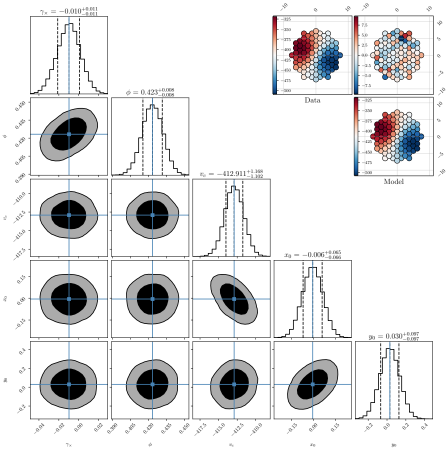

Figure 23

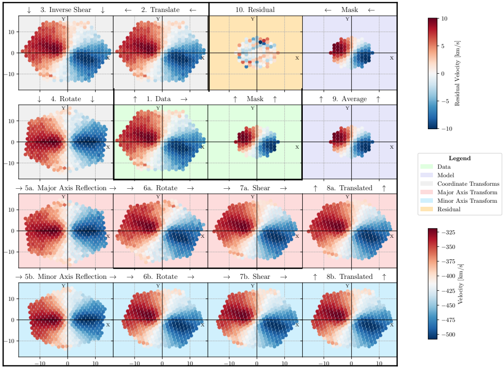

Figure 24

Galaxy Outlier Rejection

Moran's I statistic for spatial randomness in the residuals is

$$I = \frac{N}{W} \frac{\sum_i \sum_j w_{ij} \left(v_i - \bar{v}\right) \left(v_j - \bar{v}\right)}{\sum_i \left(v_i - \bar{v}\right)^2} \qquad (18)$$

A good fit is one that exhibits spatial randomness, corresponding to an I-value near zero, so $p > 0.001$

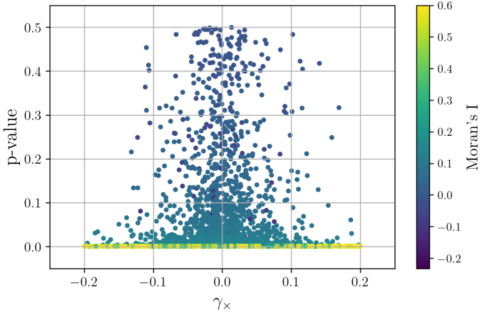

Figure 25: Moran's I and p-value per estimated cross-shear

universite PARIS-SACLAY
FACULTÉ DES SCIENCES D'ORSAY

Classification of MaNGIA Galaxies

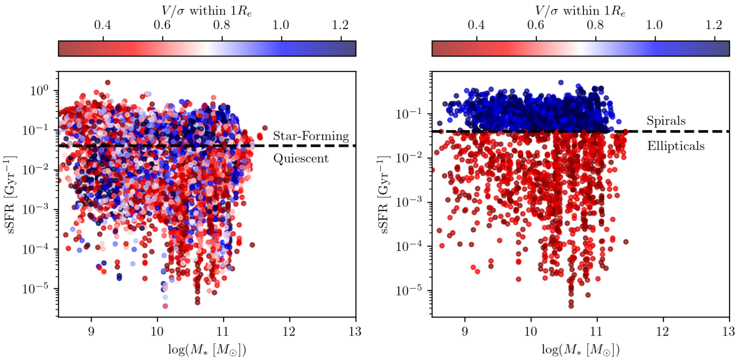

Figure 26: All the 10044 MaNGIA galaxies are positioned in the plane based on their specific star formation rate, sSFR (in Gyr^{-1}), and their total stellar mass M_* (in $M_\odot$). The colour indicates the value of the ratio between the weighted rotational velocity and the weighted velocity dispersion, V/σ.

Thank you for your attention!

References

[1] C. Hopp and D. Wittman, "Improving Precision in Kinematic Weak Lensing with MIRoRS: Model-Independent Restoration of Reflection Symmetries,", Sep. 2024. arXiv: 2410.00098 [astro-ph.CO].

[2] E. Emsellem, M. Cappellari, D. Krajnovi, *et al.*, "The SAURON project - IX. A kinematic classification for early-type galaxies," *Monthly Notices of the Royal Astronomical Society*, vol. 379, no. 2, pp. 401–417, Jul. 2007. DOI: 10.1111/j.1365-2966.2007.11752.x. [Online]. Available: https://doi.org/10.1111/j.1365-2966.2007.11752.x.

[3] ESA, *What Euclid will measure: Weak lensing*, May 2023. [Online]. Available: https://www.esa.int/ESA_Multimedia/Images/2023/05/What_Euclid_will_measure_weak_lensing.